Robust control of replication initiation in the absence of DnaA-ATP ⇋ DnaA-ADP regulatory elements in *Escherichia coli*

Thias Boesen[1]*, Godefroid Charbon[1]*, Haochen Fu[2]*, Cara Jensen[2]*, Dongyang Li[3]*, Suckjoon Jun[2,4]**, Anders Lobner-Olesen[1]**

1. Department of Biology, Center for Peptide-Based Antibiotics, University of Copenhagen, Copenhagen, Denmark

2. Department of Physics, University of California San Diego, La Jolla, CA, USA

3. Department of Biology, California Institute of Technology, Pasadena, CA, USA

4. Department of Molecular Biology, University of California San Diego, La Jolla, CA, USA

* These authors contributed equally to this work

** co-corresponding authors: suckjoon.jun@gmail.com (SJ); lobner@bio.ku.dk (ALO)

SUMMARY

Replication initiation, especially the widely conserved master initiator protein DnaA, is one of the most well-studied biological problems in bacteria. Specifically, conversion between the ATP and ADP form of DnaA during growth is critical for initiation control. In *Escherichia coli*, the regulatory elements for conversion have been discovered and extensively characterized over decades. However, they are not widely conserved in bacteria, raising questions on how to generalize the findings in *E. coli* to other organisms. In this work, we show that the intrinsic ATPase activity of DnaA itself is sufficient for robust and precise initiation control. We constructed and studied *E. coli* mutants lacking the extrinsic control of either DnaA-ATP → DnaA-ADP (by *hda* and *datA*) or DnaA-ADP → DnaA-ATP (by DARS1 and DARS2) at the single-cell and population levels. These cells showed distinct and opposing characteristics in initiation timing, the degree of initiation asynchrony, and cell-to-cell variability. Strikingly, when all four regulatory elements were deleted, *E. coli* exhibited a near wild-type phenotype, with only mildly increased intrinsic and extrinsic initiation noise. By further characterizing the DnaA variants with increased and decreased ATPase activity, we conclude that DnaA is the only requirement for robust initiation, shedding new evolutionary light on cell-cycle control in bacteria.

Introduction

Initiation of chromosome replication is a tightly regulated process, timely coordinated with growth and cell division. Indeed, cell size at initiation exhibits one of the tightest distributions, with the coefficient of variation (CV) being at most 10%, significantly smaller than other physiological variables that span over CV = 20% in *E. coli* and *Bacillus subtilis* [1–5]. Both organisms also initiate chromosome replication at a remarkably constant cell size per origin, termed the initiation mass, over a wide range of growth conditions; for example, the initiation mass varies at most 20% over a 10-fold range of the growth rate in *E. coli* [5–8].

The molecular biology of the initiation process in *E. coli* has been extensively studied. Replication initiates from a single origin, *oriC*, by binding the main initiator protein, DnaA. As an AAA+ ATPase [9], DnaA can be in either DnaA-ATP (active form) or DnaA-ADP (inactive form) with different binding affinity to DNA. For example, *oriC* contains high- and low-affinity DnaA binding sites at DAR (DnaA assembly region) (Figure 1). Both DnaA-ATP and DnaA-ADP can bind to the high-affinity sites, but only DnaA-ATP can bind to the low-affinity sites [10,11]. As DnaA-ATP molecules bind to DAR, they oligomerize and form a helical filament. The tension generated during this process results in a duplex opening at the adjacent DUE site, allowing replisome assembly therein [12]. For these reasons, it is widely accepted that DnaA-ATP is the form of DnaA required for initiation, and the conversion between DnaA-ATP and DnaA-ADP is crucial to understanding the regulation of initiation.

So far, several factors for the DnaA-ADP ⇋ DnaA-ATP conversion have been discovered (Figure 1.1). For DnaA-ADP -> DnaA-ATP, DARS1 and DARS2 (DnaA rejuvenating sequences 1 and 2) have been characterized [13]. For DnaA-ATP -> DnaA-ADP, two extrinsic mechanisms are known: RIDA (regulatory inactivation of DnaA) mediated by Hda and the DNA-loaded β-sliding clamps [14], and DDAH (*datA*-dependent DnaA-ATP hydrolysis) mediated at the five DnaA boxes at the *datA* locus [15].

The remarkable constancy of initiation mass, additionally constrained by the fundamental requirement that each replication origin fires once, and only once, per division cycle, has been a long-standing question in the field and produced several models for the role of DnaA on initiation. In general, these models assume replication initiates once the cell accumulates (1) a threshold number (not concentration) of DnaA [1,5,16,17] or (2) a threshold [DnaA-ATP]/[DnaA-ADP] ratio [18,19]. These models assume balanced biosynthesis of *dnaA* such that the overall cellular concentration of DnaA is nearly constant during the cell elongation. These models are not mutually exclusive, but their unification has challenged experiments and modelers (see [19] and references therein).

The primary purpose of the present study is to test the above two models experimentally by systematically controlling the expression level of *dnaA* and eliminating extrinsic DnaA-ADP ⇋ DnaA-ATP conversion regulatory elements. To this end, we multiplexed the original mother machine [20] to test multiple strains in the same microfluidic device (Figure 1.2). We also developed an analysis framework to distinguish and quantify the degree of initiation asynchrony within the same cell vs. cell-to-cell variability (Figure 1.3).

The most salient discovery in this report is that initiation in *E. coli* is robust even in the absence of all extrinsic DnaA-ADP ⇋ DnaA-ATP controls, and DnaA and its intrinsic ATPase activity alone is the main controller of robust initiation. These findings are general and have clear evolutionary meaning with potential applications for building synthetic cells.

Results

Quantifying asynchrony (intrinsic noise) vs. cell-to-cell variability (extrinsic noise) in initiation

One of the main goals of the present study is to differentiate the impact of initiation mutants on *synchrony* and *cell-to-cell variability* (Figure 1.2). For example, wild-type cells generally show highly synchronized initiation (Figure 1.4, left), even when the initiation mass can vary significantly from cell to cell. In some initiation mutants that we detail below, two replication origins in the same cell can fire at very different times (Figure 1.4, right).

Unfortunately, asynchrony and cell-to-cell variability cannot be easily quantified in standard flow-cytometry experiments, as both contribute to the final DNA-content distribution. Similarly, the distribution of initiation mass from single-cell experiments also reflects both noise sources.

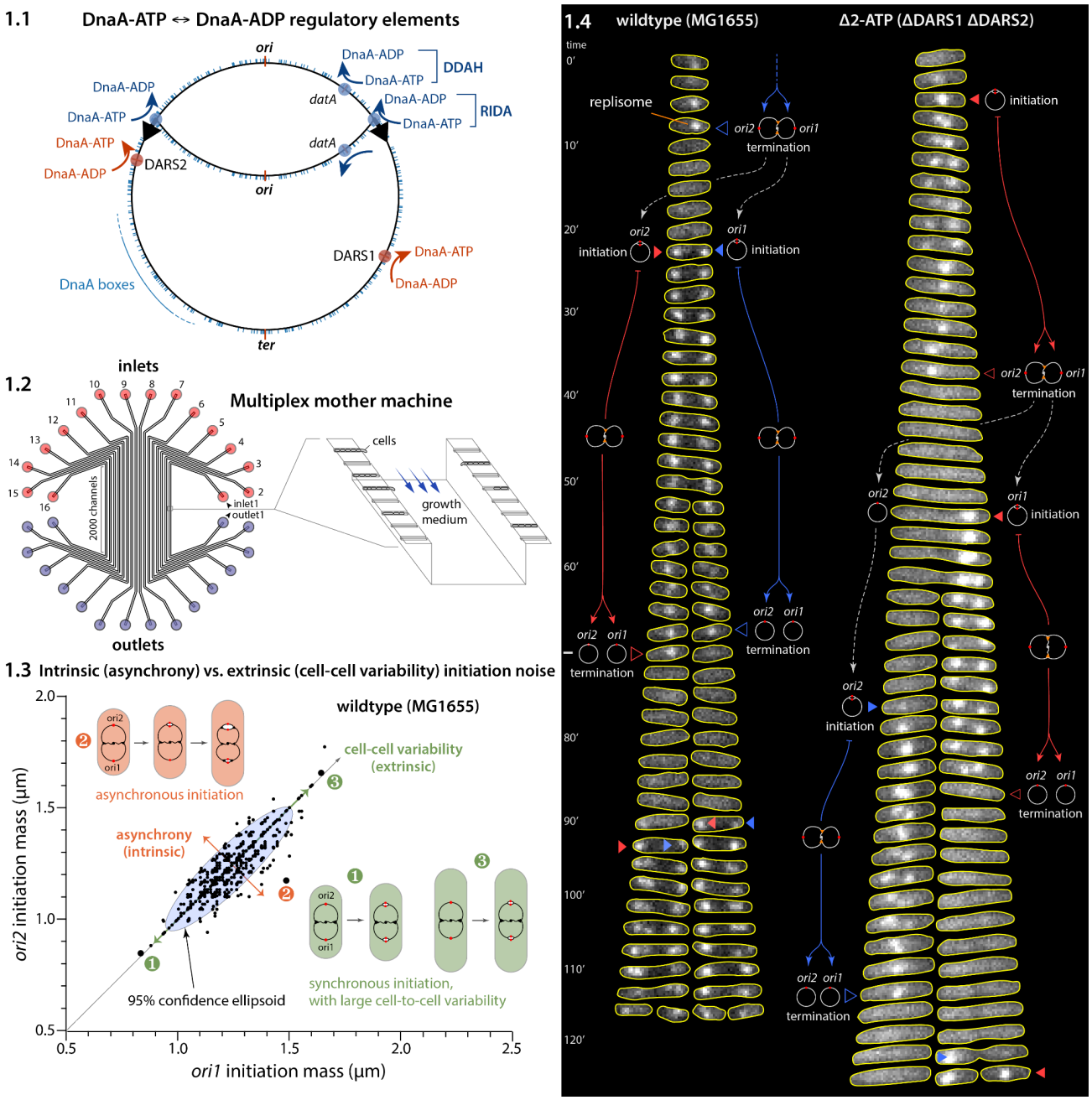

Figure 1. Experimental and analysis framework. (**1.1**) The four extrinsic DnaA-ATP ⇋ DnaA-ADP conversion regulatory elements. Based on this, we constructed Δ2-ATP (ΔDARS1 ΔDARS2), Δ2-ADP (Δ*hda* Δ*datA*), and Δ4 (ΔDARS1 ΔDARS2 Δ*hda* Δ*datA*). (**1.2**) multiplex mother machine (**1.3**) Implementing the intrinsic and extrinsic noise framework to analyze initiation asynchrony vs. cell-to-cell variability. (**1.4**) Tracking the replication dynamics using fluorescently-labeled replisomes. The wild-type cells initiate synchronously, whereas Δ2-ATP shows significant asynchrony.

However, when two replication cycles overlap, the initiation of two replication origins is analogous to the expression of two identical genes located in the left and right chromosome arms at the same genomic distance from the replication origin. Elowitz and colleagues originally devised the idea to introduce the concept of intrinsic vs. extrinsic noise in gene expression [21]. Using this analysis framework, we can plot the initiation mass of *ori*1 against *ori*2. Then, the spread along the diagonal axis is analogous to the extrinsic noise from cell-to-cell variability, whereas the stretch along the off-diagonal axis represents the initiation asynchrony or intrinsic noise (Figure 1.3). Their relative contributions to the initiation noise can be quantified independently using the same calculation scheme for intrinsic vs. extrinsic noise [21] (see Materials and Methods).

DnaA-ATP ⟶ DnaA-ADP and DnaA-ADP ⟶ DnaA-ATP have opposing effects on initiation

We first set out to examine the impact of the extrinsic DnaA-ADP ⟶ DnaA-ATP vs. DnaA-ATP ⟶ DnaA-ADP regulatory element on initiation mass and noise. We constructed and tested two types of *E. coli* strains: Δ2-ATP has ΔDARS1 and ΔDARS2, thus cannot convert DnaA-ADP ⟶ DnaA-ATP. The cells, therefore, have a lower [DnaA-ATP] and DnaA-ATP/DnaA-ADP ratio than wild-type cells [11,13]. By contrast, the Δ2-ADP (= Δ*hda* + Δ*datA*) cannot *extrinsically* stimulate the ATPase activity of DnaA, with a lower rate of DnaA-ATP ⟶ DnaA-ADP conversion compared to the wildtype. Consequently, the Δ2-ADP cells exhibit a higher level of DnaA-ATP and the DnaA-ATP/DnaA-ADP ratio [15].

The single-cell initiation data show stark differences between Δ2-ATP vs. Δ2-ADP. On the one hand, Δ2-ATP exhibits a significant delay in initiation with an increase in asynchrony (Figures 2.1 and 1.4). On the other hand, Δ2-ADP initiates prematurely (thus, at a smaller initiation mass) with almost a 3x increase in cell-to-cell variability (Figure 2.2). The flow-cytometry data are consistent with the single-cell data (Figures 2.1 and 2.2).

***E. coli* shows a near wild-type phenotype when all four DnaA-ATP ⇋ DnaA-ADP regulatory elements are deleted in Δ4**

Based on the opposing effects on initiation mass and noise observed in Δ2-ATP (ΔDARS1 ΔDARS2) and Δ2-ADP (Δ*hda* Δ*datA*), we wondered if the cells would be viable if we deleted all four control elements DARS1, DARS2, *hda*, and *datA*. Such attempts had never been made before, probably because of the apparent importance of DnaA-ADP ⇋ DnaA-ATP in initiation control. Indeed, deletion of each of these elements typically impacts the cells adversely, as seen in Figures 1.4, 2.1, and 2.2.

To our surprise, however, the Δ4 (ΔDARS1 ΔDARS2 Δ*hda* Δ*datA*) cells were not only viable but also exhibited a near wild-type initiation phenotype. Specifically, the average initiation mass remained virtually identical to the wild-type cells, with a modest increase in the CV of the initiation mass from 9.4% to 16.0% (Figure 2.3). This is consistent with the flow-cytometry data, which shows a small peak for three chromosomes representing at most a 10% increase from the control strain.

These results suggest that the rate of DnaA-ADP ⟶ DnaA-ATP by DARS1 + DARS2 and DnaA-ATP ⟶ DnaA-ADP by *hda* + *datA* (RIDA and DDAH) must be comparable to each other in the wild-type cells. In the Δ4 cells, their opposing effects largely cancel out, only mildly compromising the precision of the initiation processes.

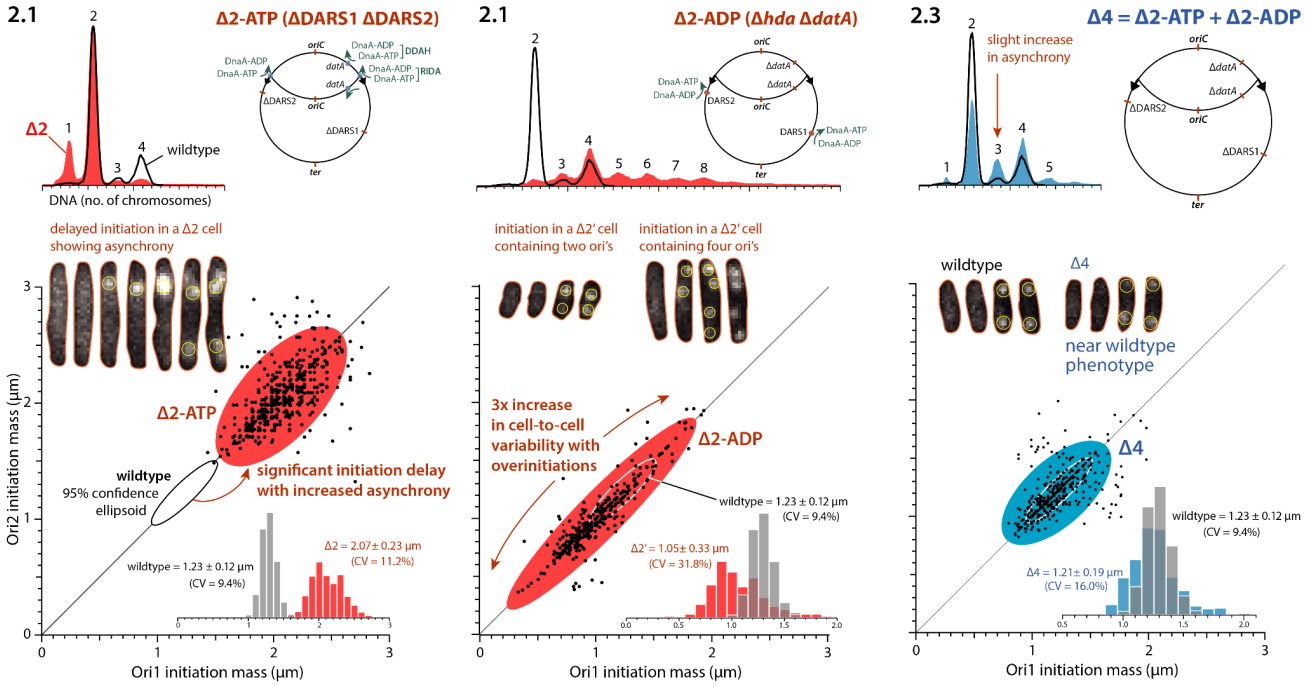

Figure 2. *E. coli* initiates robustly with DARS1, DARS2, *hda*, and *datA* deleted. (**2.1**) Δ2-ATP vs. (**2.2**) Δ2-ADP (**2.3**) Δ4.

Intrinsic ATPase activity of DnaA is sufficient for robust initiation control

If all the extrinsic regulators of DnaA-ADP ⇋ DnaA-ATP conversion are dispensable, how can *E. coli* initiate replication robustly as in the wild-type cells? We realized that the only remaining regulatory element is the DnaA itself with its intrinsic ATPase activity [9], which must be sufficient for Δ4 cells to behave like wild-type cells. To show this, we gradually overproduced wild-type DnaA ($DnaA^{WT}$) in the Δ4 background. The rationale is that, if Δ4 cells can tolerate the additional DnaA, the DnaA's ATPase activity must be sufficient for the cells to be viable without the extrinsic DnaA-ATP → DnaA-ADP conversion elements (Hda or *datA*).

The results of $DnaA^{WT}$ overproduction are shown in Figure 3.1. Up to 6x the wild-type level of DnaA we tested, the Δ4 cells were still viable. Meanwhile, they over-initiated modestly, similar to the wild-type cells (to be discussed in more detail below in Figure 4). Overall, Δ4 behaves like a wildtype with or without $DnaA^{WT}$ overproduction, indicating the ATPase activity of DnaA is sufficient for wildtype-like robust initiation control.

We also investigated two well-characterized DnaA variants in the Δ4 background. $DnaA^{R334A}$ is known for a significantly decreased ATPase activity [22], whereas $DnaA^{T174P}$ for an increased activity [23]. The $DnaA^{R334A}$ strain shows over-initiations in the flow-cytometry data, consistent with an alleviated level of [DnaA-ATP] (Figure 3.2). At the highest $dnaA^{R334A}$ induction level, we observed severely compromised replication and replication initiation, presumably because $DnaA^{R334A}$ overwhelmed $DnaA^{WT}$.

As for the fast ATPase $DnaA^{T174P}$ variant, we did not detect any noticeable changes in the average initiation mass at low to intermediate overproduction, likely because DnaA-ATP → DnaA-ADP in Δ4 was already sufficient for a stable replication cycle (Figure 3.3). Eventually, cell-to-cell variability increased when $DnaA^{T174P}$ was strongly overproduced (Figure 3.3 and SI). This might be due to the contiguous production of DnaA-ATP and the formation of short DnaA-ADP oligomers following the *de novo* synthesis of $DnaAT^{174P}$, making them unable to compete with DnaA-ATP for initiation in this strain [24].

These results underscore that the intrinsic ATPase activity is sufficient for the observed wild-type phenotype of Δ4.

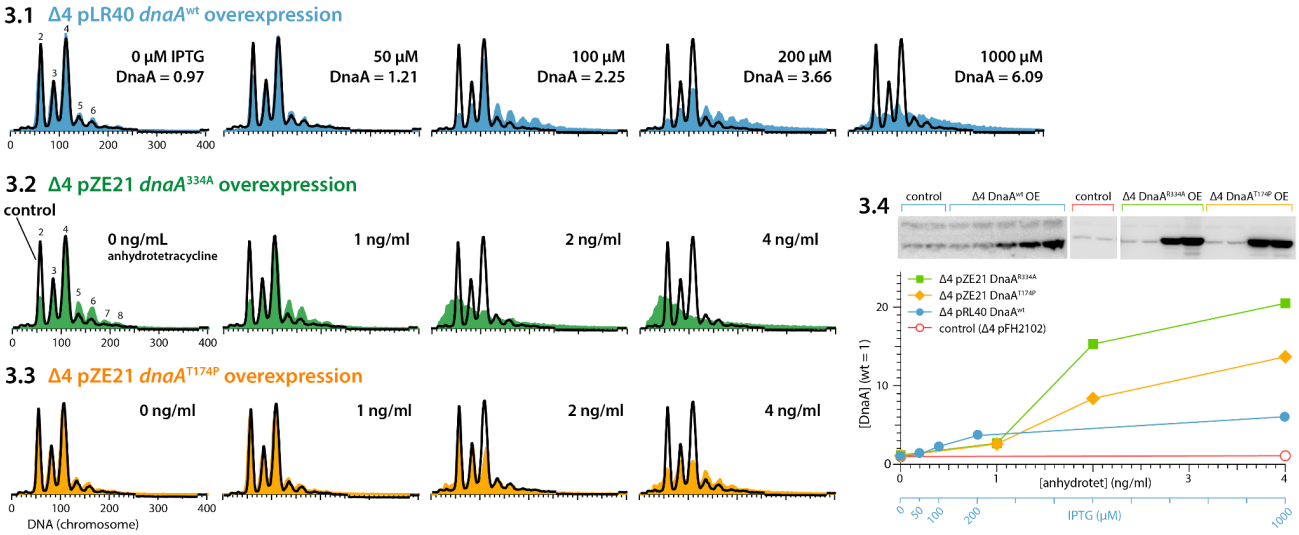

Figure 3. ATPase activity of DnaA is sufficient for robust initiation. Over-production of $DnaA^{WT}$ (**3.1**), $DnaA^{334A}$ (**3.2**), and $DnaA^{T174P}$ (**3.3**) in the Δ4 cells.

The initiation mass is inversely proportional to the *dnaA* expression level near the wildtype level

So far, we have mainly focused on the effect of DnaA-ATP ⇋ DnaA-ADP on initiation. However, the expression level of *dnaA* also clearly affects the initiation mass (Figure 4). Most previous studies on the relationship between DnaA concentration and initiation mass used a plasmid-based high *dnaA* over-expression system (Figure 3) [25–28]. For underexpression, we previously used our tCRISPRi system for gradient knockdown from the wildtype expression level [5,29], and our results were later confirmed by another study [30] (Figure 4).

For the present study, we wanted to fine-control the *dnaA* expression level from 50% to 200% of the wildtype level by replacing the endogenous *dnaA* with the inducible version. However, for reasons that were not clear

to us initially, we found no such system and thus set out to construct one. We chose the pBAD* expression system we developed for tCRISPRi for its titratability and uniform expression distribution [29], but the cloning was challenging. We first introduced an additional copy of *dnaA* under the araBAD promoter to build such a strain. We then attempted to delete the endogenous *dnaA* but consistently failed because the deletion was lethal for the cells. After many failed attempts, we realized that the expression of pBAD*::*dnaA* was insufficient to maintain cell viability since *dnaA* is an essential gene with a high expression level, an indicator that *dnaA* expression level matters for the cell. In particular, the inducible promoter suffered from catabolic repression in fast-growth conditions, the standard growth conditions for cloning. Eventually, we solved the problem using two different methods, which enabled us to probe the expression level around the wild-type level, as presented in the following sections. Please see Materials and Methods for a more detailed description.

Shown in Figure 4 is the *dnaA* expression level vs. initiation mass from this study, overlaid with data from all previous studies we could find [5,27–31]. Notably, when *dnaA* was underexpressed, the initiation delayed, and the initiation mass increased sharply, inversely proportional to the *dnaA* expression level. These results are consistent with previous reports mentioned above [5,29,30].

The same inverse trend persisted at mild overexpression up to the 2x wild-type level (Figure 4). As the expression level continued to increase, the initiation mass reached a plateau [27]. Nevertheless, the data show a clear trend that the expression level of *dnaA* does affect the initiation mass, mostly inverse proportional to the *dnaA* expression level.

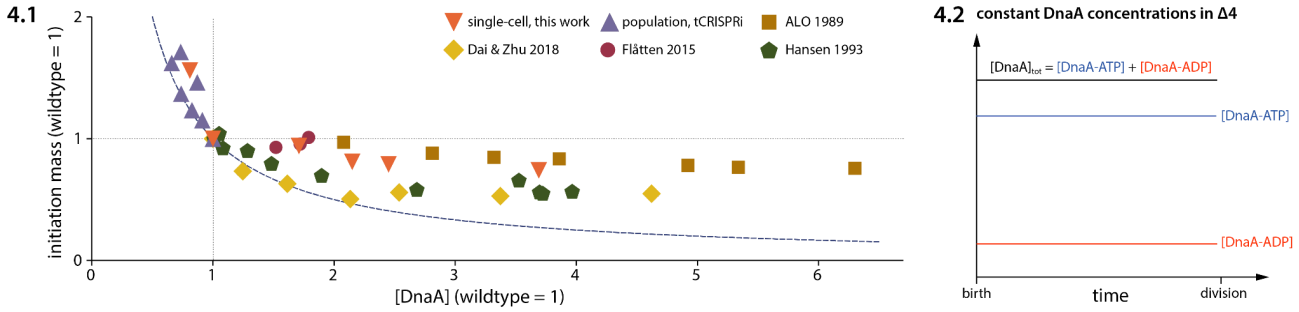

Figure 4. DnaA concentration and initiation mass. (**4.1**) The average initiation mass is inversely proportional to the expression level of *dnaA*. The average initiation mass reaches a plateau at high *dnaA* expression (> 2x the wild-type level). (**4.2**) The concentration of DnaA, DnaA-ATP, and DnaA-ADP must be constant in Δ4 strain during cell elongation.

Discussion and conclusion

In this work, we have shown that *E. coli* can control replication initiation robustly with all known extrinsic regulatory elements for DnaA-ATP ⇋ DnaA-ADP conversion, DARS1, DARS2, *hda*, and *datA* deleted. How is the intrinsic ATPase activity of DnaA sufficient for regulation of initiation, and which initiation model is consistent with our results?

First of all, the most critical quantitative insight from Δ4's wild-type behavior is that the DnaA-ATP/DnaA-ADP ratio cannot determine the initiation timing (Figure 4.2). In the balanced biosynthesis of DnaA [1,16,19] (SI), the number of DnaA-ATP, N_{ATP}, can be described by $dN_{ATP}/dt = \lambda N_{tot} - \nu N_{ATP}$ and $dN_{tot}/dt = \lambda N_{tot}$, where N_{tot} is the total number of DnaA and λ the growth rate. The steady-state solution of these equations leads to [DnaA] = constant, [DnaA-ATP] = constant, and [DnaA-ADP] = constant during cell elongation (Figure 5.1). This directly refutes any initiation model based on DnaA concentrations or their ratios, such as [DnaA-ATP]/[DnaA-ADP].

What, then, is the correct model of initiation? One, periodic initiation must rely on the oscillations of a "factor" at the same frequency as cell division and, two, the "factor" must be related to DnaA-ATP. The simplest model, therefore, requires the "factor" to be the *number* of DnaA-ATP, not the *concentration* of DnaA-ATP. Then, initiation is triggered when each origin accumulates a fixed threshold number of DnaA-ATP, analogous to the threshold of FtsZ number required for cell division [1]. The balanced production of DnaA and the threshold imposed on the DnaA-ATP copy number naturally leads to the adder principle [1] as well as the 1/[DnaA] dependence of the average initiation mass in Figure 4 (SI).

A new emerging picture from this study and the bacterial cell-size control [1] is that the bacterial cell cycle control must depend on the copy-number sensing mechanism. This puts the bacterial cell cycle control in a profoundly different place from the concentration-based eukaryotic cell-cycle control, wherein the cell-cycle regulators are periodically expressed and degraded/diluted [32]. We are currently working on the full model that can also quantitatively explain the origin of asynchrony and cell-to-cell variability reported in this work.

Finally, the robust initiation of the Δ4 cells and its mechanistic implications was a major surprise for us. At the same time, we also find them gratifying from an evolutionary perspective [33,34]. For example, the First Cell would only need one master regulator protein with intrinsic ATPase activity for robust initiation, and different organisms may have acquired organism-specific additional control mechanisms to improve the precision in initiation during evolution (Figure 2). While modest in the cell-cycle timescale, their impact on the evolutionary timescale is unquestionable.

Materials and Methods

Growth Conditions

Cells were grown in Lysogeny Broth (LB) or AB minimal medium (Clark & Maaløe, 1967) supplemented with 10 µg/mL thiamine and either 0.2% glycerol (ABT-Glycerol) or 0.2% glucose (ABT-Glucose). When necessary, antibiotics were added in the following concentrations: kanamycin, 50 µg/mL, chloramphenicol, 20 µg/mL, ampicillin, 150 µg/mL.

Strains

Construction and measurement of the *dnaA*-inducible strains. We made the inducible *dnaA* strain (SJ1499) by first introducing an extra copy of *dnaA* with a co-transcriptional reporter msfGFP under the *araBAD* promoter to SJ_XTL175 using recombineering. We next introduced a replisome marker (*mCherry-dnaN*) with a kanamycin selection marker (*kan*) to generate an intermediate strain SJ1496. The endogenous *dnaA* locus was further replaced with a chloramphenicol selection marker (*cat*) using recombineering to generate the *dnaA* titration strain SJ1499.

As mentioned in the main text, *dnaA* is an essential gene with a strong promoter. Using an inducible promoter can pose difficulties in cloning due to catabolic repression. Indeed, many failed attempts prompted us to question whether the expression of pBAD*::*dnaA* is sufficient to maintain cell viability. To test this, we used a GFP inducible strain (pBAD*::*msfGFP*) to measure the expression level from the araBAD promoter. Expression from pBAD* is highly suppressed in LB or other rich media (data not shown). Two reasons prevent the expression of pBAD*: 1) araBAD promoter is susceptible to catabolite repression. Cells growing in rich media like LB or glucose have very low amounts of cAMP, hence minimal expression from CRP-dependent promoters, including pBAD [35]. 2) the pBAD* system relies on the lacY (A177C) to transport the inducer arabinose into cells. The lacY (A177C) is expressed from its endogenous lacI promoter, which also relies on CRP. As a result, both the pBAD* expression and transportation of its inducer are limited in low-cAMP conditions. This led to the little expression of pBAD*::*dnaA* in standard cloning procedures using LB-based media.

We successfully employed two different methods to solve this issue of insufficient expression. In the first method, we replaced the promoter of *lacY* (A177C) with a constitutive high-expressing promoter, pLacIq1. This alleviates the restriction on arabinose import. This new expression system (pBAD**) showed a ~2-fold increase in GFP expression levels in its titratable range in low cAMP growth regime (MOPS glucose), whereas expression level does not change in high cAMP growth regime (MOPS glycerol) (Figure 1). The pBAD** allowed us to make a *dnaA*-inducible strain. In the second method, we used pBAD* but bypassed its catabolic repression by growing cells in slow growth conditions (M9 glycerol or MOPS glycerol) throughout the cloning process. Both methods allowed us to maintain sufficient *dnaA* expression levels during the cloning procedure.

For our *dnaA* titration experiment, we chose the pBAD*::*dnaA* over pBAD**:*dnaA* for its range of expression in minimal MOPS glucose media in our experiments in Figure 4; the endogenous *dnaA* expression level lies at ~50% induction level in pBAD*, whereas the new pBAD** system has a higher expression level.

We quantified the DnaA concentration using a co-transcriptional reporter msfGFP. We measured the initiation mass using a replisome marker from time-lapse fluorescence imaging with the mother machine (mCherry-dnaN, [1])

Construction of Δ2-ATP, Δ2-ADP, and Δ4 strains. All strains used were derivatives of *E. coli* K-12 MG1655 (F- λ- *rph*-1) [36]. All deletions were performed by P1-mediated transduction(Miller, 1972). The Δ*hda* Δ*datA* strain was constructed by transducing Δ*hda* into a Δ*datA* strain and plating it on an ABT-Glycerol medium as described previously [37,38]. The individual Δ*DARS1:cat* (ALO4313) and Δ*DARS2:cat* (ALO4254) mutants were constructed previously [39,40] using the λ-red procedure [41]. Before combining the Δ*DARS1* and Δ*DARS2*, the *cat* resistance marker was cured from ALO4313 using pCP20 [42]. The Δ*4* strain (Δ*DARS1* and Δ*DARS2* Δ*hda* Δ*datA*) was constructed by combining the above by P1 transduction. All strains were whole genome sequenced to confirm the presence of the mutations and to ensure that no suppressors appeared.

To track the initiation of chromosome replication in the strains, we used a fluorescently labeled sliding-clamp of the replisome, DnaN-YPet, as described previously [1,43].

Plasmids. We constructed plasmid pZE21DnaA by amplification of dnaA using primers AAGGTACCGTGTCACTTTCGCTTTGGCAGCAGTGTCTTGCCCGATTGC and GGAAGCTTTTACGATGACAATGTTCTGATTAAATTTGAAAAATCTTCT.

The amplicon and plasmid pZE21 [44] were cut with restriction enzymes KpnI and HindIII, and then ligated to create pZE21DnaA. pZE21 DnaA^{R334A} was created using primers AAGGTACCGTGTCACTTTCGCTTTGGCAGCAGTGTCTTGCCCGATTGC, GGAAGCTTTTACGATGACAATGTTCTGATTAAATTTGAAAAATCTTCT, TCGCCAAGCGTCTACGATCTAACG TAGCTGAGCTGGAAGGGGCGCTGAAC, and GTTCAGCGCCCCTTCCAGCTCAGCTACGTTAGATCGTAGACGCTTGGCGA.

pZE21 DnaAT^{174P} was created using primers AAGGTACCGTGTCACTTTCGCTTTGGCAGCAGTGTCTTGCCCGATTGC, GGAAGCTTTTACGATGACAATGTTCTGATTAAATTTGAAAAATCTTCT, ATGGCGGCCCGGGTCTGGGTAAAACTCACC, and ACCCAGACCCGGGCCGCCATAAAGGAACAA.

Flow cytometry

Cells were balanced in exponential growth for more than 10 generations and incubated with 300 µg/mL rifampicin and 36 µg/mL at 37°C for 4 hours, allowing ongoing replication cycles to terminate. Cells were harvested and resuspended in 100 µL 10mM Tris-HCl, pH 7.4, and fixed by adding 1 mL of 77% ethanol and stored at 4°C.

Before flow cytometric analysis, fixed cells were pelleted by centrifugation at 15,000 x g for 15 min. The supernatant was discarded, and the pellet was resuspended in 150 µl staining solution (90 µg/mL mithramycin, 20 µg/mL ethidium bromide, 10 mM $MgCl_2$, 10 mM Tris-HCl, pH 7.4). Samples were kept on ice for a minimum of 10 minutes before analysis.

We performed flow cytometry experiments as described previously [27] using an Apogee A10 system. A minimum of 30,000 cells for each sample were analyzed, and the number of origins per cell and relative mass were determined as described previously [27].

Microfluidics

We used PDMS-based mother machines to track single-cell lineages. To guarantee the same experimental conditions for control experiments, we designed duplex mother machines and multiplex mother machines that contain two main trenches and sixteen main trenches on each device, respectively. Each side of the main trench consists of 2000 channels with a width ranging from 1.1 um to 1.5 um in design. The inlet of each main trench was connected to a syringe with a growth medium by Teflon tubing. The syringes were controlled by syringe pumps (PHD Ultra, Harvard Apparatus, MA) to maintain a constant flow rate.

Cell preparation

A single colony was inoculated in 1 mL ABT-Glucose, containing appropriate antibiotics, and incubated overnight at 37°C in a water-bath shaker. Cells were then diluted 1000-fold into fresh media and balanced in an exponential phase for more than 10 generations. When reaching an OD_{450} of 0.1-0.15, cells were pelleted, concentrated, and injected into the mother machine device prewashed with BSA to reduce cell adhesion in the device channels. A constant flow of fresh growth media was supplied through the device for the duration of the experiment, as described previously [1,45].

Microscopy

We performed phase contrast and fluorescence imaging tandemly on an inverted microscope (Nikon Ti-E) with Perfect Focus 3 (PFS3), 100x oil immersion objective (PH3, numerical aperture = 1.45), Obis lasers 488LX (Coherent Inc., CA) as fluorescence light source, Chroma EYFP filter (49003-ET-EYFP), and Prime 95B sCMOS camera (Photometrics) [1]. The laser power for 488 nm excitation was 30 mW, and the exposure time was 100 ms. The imaging time interval was 2.5 min for all the mother machine experiments.

Image analysis

We followed the developed protocol of mother machine image analysis (mm3) [46]. For cell segmentation, we used a machine-learning-based method, U-net, rather than the traditional Otsu method to obtain more reliable results [47]. For fluorescence foci identification, we used a Laplacian of Gaussian method [1]. The foci intensity and position were recorded and replotted against time for a whole cell lineage in Matlab. The start point and the end point of each foci trace were considered as the initiation point and the termination point, respectively. To avoid any aging effects in some mother cells, we only tracked the first daughter cells (namely, the top daughter cell of a bottom mother cell). The cell length at the initiation point is recorded, and the initiation mass is defined as the cell length at initiation divided by the the number of origins given the negligible change in cell width.

Quantification of the initiation noise

Once we obtained a list of initiation mass for *ori*1 and for *ori*2, defined as *x* and *y*, we can calculate the extrinsic initiation noise, the intrinsic initiation noise, and the total initiation noise in the similar way as Elowits et al. (19):

$$CV_{int}^2 = \frac{<(x-y)>^2}{2<x><y>}, CV_{ext}^2 = \frac{<xy>-<x><y>}{<x><y>}, CV_{tot}^2 = CV_{int}^2 + CV_{ext}^2,$$

where the "<>" means taking the average value.

References

1. Si F, Le Treut G, Sauls JT, Vadia S, Levin PA, Jun S. Mechanistic Origin of Cell-Size Control and Homeostasis in Bacteria. Curr Biol. 2019;29: 1760–1770.e7.
2. Sauls JT, Cox SE, Do Q, Castillo V, Ghulam-Jelani Z, Jun S. Control of Bacillus subtilis Replication Initiation during Physiological Transitions and Perturbations. MBio. 2019;10. doi:10.1128/mBio.02205-19
3. Wallden M, Fange D, Lundius EG, Baltekin Ö, Elf J. The Synchronization of Replication and Division Cycles in Individual E. coli Cells. Cell. 2016;166: 729–739.
4. Knöppel A, Broström O, Gras K, Fange D, Elf J. The coordination of replication initiation with growth rate in Escherichia coli. bioRxiv. 2022. p. 2021.10.11.463968. doi:10.1101/2021.10.11.463968
5. Si F, Li D, Cox SE, Sauls JT, Azizi O, Sou C, et al. Invariance of Initiation Mass and Predictability of Cell Size in Escherichia coli. Curr Biol. 2017;27: 1278–1287.
6. Donachie WD. Relationship between cell size and time of initiation of DNA replication. Nature. 1968;219: 1077–1079.
7. Wold S, Skarstad K, Steen HB, Stokke T, Boye E. The initiation mass for DNA replication in Escherichia coli K-12 is dependent on growth rate. EMBO J. 1994;13: 2097–2102.
8. Zheng H, Bai Y, Jiang M, Tokuyasu TA, Huang X, Zhong F, et al. General quantitative relations linking cell growth and the cell cycle in Escherichia coli. Nat Microbiol. 2020;5: 995–1001.
9. Sekimizu K, Bramhill D, Kornberg A. ATP activates dnaA protein in initiating replication of plasmids bearing the origin of the E. coli chromosome. Cell. 1987;50: 259–265.
10. Leonard AC, Grimwade JE. Regulation of DnaA assembly and activity: taking directions from the genome. Annu Rev Microbiol. 2011;65: 19–35.
11. Riber L, Frimodt-Møller J, Charbon G, Løbner-Olesen A. Multiple DNA Binding Proteins Contribute to Timing of Chromosome Replication in E. coli. Front Mol Biosci. 2016;3: 29.
12. Erzberger JP, Mott ML, Berger JM. Structural basis for ATP-dependent DnaA assembly and replication-origin remodeling. Nat Struct Mol Biol. 2006;13: 676–683.
13. Fujimitsu K, Senriuchi T, Katayama T. Specific genomic sequences of E. coli promote replicational initiation by directly reactivating ADP-DnaA. Genes Dev. 2009;23: 1221–1233.

14. Kato J, Katayama T. Hda, a novel DnaA-related protein, regulates the replication cycle in Escherichia coli. EMBO J. 2001;20: 4253–4262.

15. Kasho K, Katayama T. DnaA binding locus *datA* promotes DnaA-ATP hydrolysis to enable cell cycle-coordinated replication initiation. Proceedings of the National Academy of Sciences. 2013;110: 936–941.

16. Sompayrac L, Maaløe O. Autorepressor Model for Control of DNA Replication. Nat New Biol. 1973;241: 133–135.

17. Hansen FG, Christensen BB, Atlung T. The initiator titration model: computer simulation of chromosome and minichromosome control. Res Microbiol. 1991;142: 161–167.

18. Donachie WD, Blakely GW. Coupling the initiation of chromosome replication to cell size in Escherichia coli. Curr Opin Microbiol. 2003;6: 146–150.

19. Berger M, ten Wolde PR. Robust replication initiation from coupled homeostatic mechanisms. bioRxiv. 2022. p. 2022.08.04.502793. doi:10.1101/2022.08.04.502793

20. Wang P, Robert L, Pelletier J, Dang WL, Taddei F, Wright A, et al. Robust Growth of Escherichia coli. Curr Biol. 2010;20: 1099–1103.

21. Elowitz MB, Levine AJ, Siggia ED, Swain PS. Stochastic Gene Expression in a Single Cell. Science. 2002;297: 1183–1186.

22. Nakamura K, Katayama T. Novel essential residues of Hda for interaction with DnaA in the regulatory inactivation of DnaA: unique roles for Hda AAA Box VI and VII motifs. Mol Microbiol. 2010;76: 302–317.

23. Gon S, Camara JE, Klungsøyr HK, Crooke E, Skarstad K, Beckwith J. A novel regulatory mechanism couples deoxyribonucleotide synthesis and DNA replication in Escherichia coli. EMBO J. 2006;25: 1137–1147.

24. Kawakami H, Keyamura K, Katayama T. Formation of an ATP-DnaA-specific initiation complex requires DnaA Arginine 285, a conserved motif in the AAA+ protein family. J Biol Chem. 2005;280: 27420–27430.

25. Atlung T, Løbner-Olesen A, Hansen FG. Overproduction of DnaA protein stimulates initiation of chromosome and minichromosome replication in Escherichia coli. Mol Gen Genet. 1987;206: 51–59.

26. Pierucci O, Helmstetter CE, Rickert M, Weinberger M, Leonard AC. Overexpression of the dnaA gene in Escherichia coli B/r: chromosome and minichromosome replication in the presence of rifampin. J Bacteriol. 1987;169: 1871–1877.

27. Løbner-Olesen A, Skarstad K, Hansen FG, von Meyenburg K, Boye E. The DnaA protein determines the initiation mass of Escherichia coli K-12. Cell. 1989;57: 881–889.

28. Atlung T, Hansen FG. Three distinct chromosome replication states are induced by increasing concentrations of DnaA protein in Escherichia coli. J Bacteriol. 1993;175: 6537–6545.

29. Li X-T, Jun Y, Erickstad MJ, Brown SD, Parks A, Court DL, et al. tCRISPRi: tunable and reversible, one-step control of gene expression. Sci Rep. 2016;6: 39076.

30. Dai Xiongfeng, Zhu Manlu. High Osmolarity Modulates Bacterial Cell Size through Reducing Initiation Volume in Escherichia coli. mSphere. 2018;3: e00430–18.

31. Flåtten I, Fossum-Raunehaug S, Taipale R, Martinsen S, Skarstad K. The DnaA Protein Is Not the Limiting Factor for Initiation of Replication in Escherichia coli. PLoS Genet. 2015;11: e1005276.

32. Hunt T, Murray A. The cell cycle : an introduction. Oxford University Press; 1993.

33. Pelletier JF, Sun L, Wise KS, Assad-Garcia N, Karas BJ, Deerinck TJ, et al. Genetic requirements for cell division in a genomically minimal cell. Cell. 2021;184: 2430–2440.e16.

34. Olivi L, Berger M, Creyghton RNP, De Franceschi N, Dekker C, Mulder BM, et al. Towards a synthetic cell cycle. Nat Commun. 2021;12: 1–11.

35. You C, Okano H, Hui S, Zhang Z, Kim M, Gunderson CW, et al. Coordination of bacterial proteome with

metabolism by cyclic AMP signalling. Nature. 2013;500: 301–306.

36. Guyer MS, Reed RR, Steitz JA, Low KB. Identification of a sex-factor-affinity site in E. coli as gamma delta. Cold Spring Harb Symp Quant Biol. 1981;45 Pt 1: 135–140.

37. Charbon G, Klitgaard RN, Liboriussen CD, Thulstrup PW, Maffioli SI, Donadio S, et al. Iron chelation increases the tolerance of Escherichia coli to hyper-replication stress. Sci Rep. 2018;8: 1–14.

38. Riber L, Olsson JA, Jensen RB, Skovgaard O, Dasgupta S, Marinus MG, et al. Hda-mediated inactivation of the DnaA protein and dnaA gene autoregulation act in concert to ensure homeostatic maintenance of the Escherichia coli chromosome. Genes Dev. 2006;20: 2121–2134.

39. Frimodt-Møller J, Charbon G, Krogfelt KA, Løbner-Olesen A. Control regions for chromosome replication are conserved with respect to sequence and location among Escherichia coli strains. Front Microbiol. 2015;6: 1011.

40. Frimodt-Møller J, Charbon G, Krogfelt KA, Løbner-Olesen A. DNA Replication Control Is Linked to Genomic Positioning of Control Regions in Escherichia coli. PLoS Genet. 2016;12: e1006286.

41. Datsenko KA, Wanner BL. One-step inactivation of chromosomal genes in *Escherichia coli* K-12 using PCR products. Proceedings of the National Academy of Sciences. 2000;97: 6640–6645.

42. Cherepanov PP, Wackernagel W. Gene disruption in Escherichia coli: TcR and KmR cassettes with the option of Flp-catalyzed excision of the antibiotic-resistance determinant. Gene. 1995;158: 9–14.

43. Reyes-Lamothe R, Sherratt DJ, Leake MC. Stoichiometry and architecture of active DNA replication machinery in Escherichia coli. Science. 2010;328: 498–501.

44. Lutz R, Bujard H. Independent and tight regulation of transcriptional units in Escherichia coli via the LacR/O, the TetR/O and AraC/I1-I2 regulatory elements. Nucleic Acids Res. 1997;25: 1203–1210.

45. Taheri-Araghi S, Bradde S, Sauls JT, Hill NS, Levin PA, Paulsson J, et al. Cell-Size Control and Homeostasis in Bacteria. Curr Biol. 2015;25: 385–391.

46. Sauls JT, Schroeder JW, Brown SD, Le Treut G, Si F, Li D, et al. Mother machine image analysis with MM3. bioRxiv. 2019. p. 810036. doi:10.1101/810036

47. Ronneberger O, Fischer P, Brox T. U-Net: Convolutional Networks for Biomedical Image Segmentation. Medical Image Computing and Computer-Assisted Intervention – MICCAI 2015. Springer International Publishing; 2015. pp. 234–241.

48. Nozaki S, Niki H, Ogawa T. Replication initiator DnaA of Escherichia coli changes its assembly form on the replication origin during the cell cycle. J Bacteriol. 2009;191: 4807–4814.